Journal of Molecular Structure 975 (2010) 265–273

Contents lists available at ScienceDirect

Journal of Molecular Structure

journal homepage: www.elsevier.com/locate/molstruc

Effect of ligand substitution on DNA binding ability of two new square planar copper(II)–Schiff base complexes

Dipali Sadhukhan [a], Aurkie Ray [a], Saurabh Das [a], Corrado Rizzoli [b], Georgina M. Rosair [c], Samiran Mitra [a,*]

[a] Department of Chemistry, Jadavpur University, Raja S.C. Mullick Road, Kolkata 700 032, West Bengal, India
[b] Universitá degli Studi di Parma, Dipartimento di Chimica Generale ed Inorganica, Chimica Analitica, Chimica Fisica Viale, G.P. Usberti 17/A I-43100 Parma, Italy
[c] School of Engineering and Physical Sciences, Heriot Watt University, Edinburgh EH14 4AS, UK

ARTICLE INFO

Article history:
Received 16 March 2010
Received in revised form 26 April 2010
Accepted 26 April 2010
Available online 29 April 2010

Keywords:
Copper(II) complexes
Square planarity
Bifurcated H-bonding
CT-DNA
Hypochromism
Intercalation

ABSTRACT

Two terdentate NNO donor Schiff base ligands $CH_3C(OH)=CHC(CH_3)=NCH_2C_5H_4N$ [**HL^1**] and $C_6H_5C(OH)=CHC(CH_3)=NCH_2C_5H_4N$ [**HL^2**] were used to synthesize two mononuclear square planar copper(II) complexes, [Cu**L^1**(CF_3COO)] (**1**) and [Cu**L^2**(CF_3COO)] (**2**). The complexes were characterized by elemental analyses, FT-IR, UV–vis spectral methods and their structures were established by single crystal X-ray diffraction study. The biochemical activity of the complexes towards DNA binding were performed using absorbance and fluorescence titration methods and their mode of binding with calf thymus DNA has been established by viscosity measurement technique.

1. Introduction

The Schiff base metal complexes are very important tools for inorganic chemists as these are widely used to design molecular ferromagnets, in catalysis, in biological modeling applications and as liquid crystals [1]. There are numerous accounts in the literature describing the chemistry of metal complexes of Schiff base ligands containing two, three, four, five and six donor atoms [2]. Terdentate Schiff bases with NNO donor sets have been often used to block the coordination sites of metal ions which prefer square planar or square pyramidal geometry and to saturate the coordination number of the metal ion. A bridging ligand has been used to synthesize dinuclear and multinuclear complexes [3–6]. Carboxylate ligands serve this purpose well [7, 8]. Sometimes when a complex strongly prefers square-planar geometry the carboxylate anion binds in terminal monodentate fashion [9,10]. Small Schiff base ligands with N-heterocyclic aromatic ring where the hetero atom can coordinate to the metal ion are expected to induce a good extent of planarity to the complexes because of the rigidity inserted within the ligand framework by the coordinating heterocycle. Earlier our research group synthesized such planar complexes of copper(II) with terdentate NNO donor Schiff base ligands containing N-heterocyclic fragment by the condensation of 2-picolyl amine with acetyl acetone and benzoyl acetone [11,12]. Those complexes were characterized structurally, spectroscopically and magnetically but the utility of the complexes in biochemical field remained unexplored.

Planar mononuclear complexes with solubility in buffered aqueous medium can penetrate more easily through cell membrane compared to the large organic molecules and hence have gained much importance now a day to interact with DNA and to act as chemical nuclease [13–21]. Metal complexes of the ligands having planar aromatic heterocyclic ring such as pyridine, bipyridine, phenanthroline moieties are good metallointercalators [22–27] and have been employed so far in binding studies with DNA. Although a number of small inorganic complexes containing Cu^{II}, Zn^{II}, Co^{III}, Ru^{II} metal ions with varieties of ligand systems have been reported so far [28] still there are scope to design and study new complexes of the same or different metal ions with special modifications in the ligand system as new chemical nuclease. Aspired by this idea, in continuation to our earlier works [11,12] we have synthesized two new copper(II) complexes [**1** and **2**] with the terdentate NNO donor Schiff base ligands by the condensation of 2-picolyl amine with acetyl acetone [**HL^1**] and benzoyl acetone [**HL^2**]. We have designed our ligand systems [**HL^1** and **HL^2**] so that they differ only by a substituent (methyl in **HL^1** and phenyl in **HL^2**) and have monitored the effect imposed by the substituents on the structure–function relationship of respective complexes [**1** and **2**] during interaction with DNA by absorption and fluorescence

* Corresponding author. Tel.: +91 033 2414 6666x2779; fax: +91 033 2414 6414.
E-mail address: smitra_2002@yahoo.com (S. Mitra).

0022-2860/$ - see front matter © 2010 Elsevier B.V. All rights reserved.
doi:10.1016/j.molstruc.2010.04.034

titration methods. The probable modes of binding of the two complexes were investigated by viscosity measurement of the DNA in absence and in presence of the complex solutions.

In this paper we have described the crystal structures of two new square planar copper(II)–Schiff base complexes (**1** and **2**) along with spectral characterization methods and have monitored their reverberation towards interaction with calf thymus DNA by UV–vis, fluorescence and viscometric methods.

2. Experimental

2.1. Materials

All solvents were of reagent grade and used without further purification. 2-picolylamine, acetyl acetone and benzoyl acetone were purchased form Aldrich Chemical Company and were used as received. Copper trifluoroacetate hexahydrate was prepared by treatment of copper carbonate (E. Merck, India) with 60% trifluoroacetic acid (E. Merck, India) followed by the slow evaporation on the steam bath. It was then filtered through a fine glass-frit and preserved in a $CaCl_2$ desiccator for further use.

2.2. Syntheses

2.2.1. Syntheses of the Schiff base ligands (*HL¹* and *HL²*)

The Schiff base ligand (**HL¹**) was synthesized by the reflux condensation of a 25 ml methanolic solution of 2-picolylamine (0.51 ml, 5 mmol) with 25 ml methanolic solution of acetyl acetone (0.52 ml, 5 mmol). The ligand was refluxed for 2 h when a yellow solution was obtained. The colour indicated the formation of the Schiff base **HL¹** which was used without further purification.

HL² was synthesized by refluxing 25 ml methanolic solution of 2-picolylamine (0.51 ml, 5 mmol) with 25 ml methanolic solution of benzoyl acetone (0.18 gm, 5 mmol) following the same procedure as **HL¹**. The schematic representation of the syntheses of the ligands is depicted in Scheme 1.

2.2.2. Synthesis of [Cu*L¹*(CF₃COO)] (*1*)

$Cu(CF_3COO)_2.6H_2O$ (0.397 g, 1 mmol) was dissolved in 20 ml 2-propanol. 10 ml yellow methanolic solution of the Schiff base (**HL¹**) (1 mmol) was added to the former. The mixture was allowed to stir for 2 h with warming. The dark green solution was kept in refrigerator at 16 °C. Brown plate shaped single crystals suitable for X-ray diffraction were obtained within one day. Crystals were isolated by filtration and were air-dried. Yield: 0.33 g (85%). Anal. Calc. for $[C_{13}\ H_{13}\ Cu\ F_3\ N_2\ O_3]$: C, 42.65; H, 3.55; N, 7.65. Found: C, 42.69; H, 3.60; N, 7.68%.

2.2.3. Synthesis of [Cu*L²*(CF₃COO)] (*2*)

$Cu(CF_3COO)_2.6H_2O$ (0.397 g, 1 mmol) was dissolved in 5 ml methanol. 10 ml yellow methanolic solution of the Schiff base (**HL²**) (1 mmol) was added to the former in stirring condition. The mixture was allowed to stir for 2 h at room temperature. The dark green solution was kept in refrigerator at 16 °C yielding green needle shaped crystals suitable for X-ray diffraction after a week. Crystals were isolated by filtration and were air-dried. Yield: 0.32 g (80%). Anal. Calc. for $[C_{18}\ H_{15}\ Cu\ F_3\ N_2\ O_3]$: C, 50.48; H, 3.51; N, 6.54. Found: C, 50.50; H, 3.54; N, 6.57%.

2.3. Physical measurements

The Fourier Transform Infrared spectra (4000–400 cm^{-1}) of the ligands and the complexes were recorded on a Perkin–Elmer Spectrum RX I FT-IR system with solid KBr disc. The electronic spectra were recorded, in acetonitrile or in 5 mM Tris–50 mM NaCl buffer (pH ~ 7.4), on a Perkin–Elmer Lambda 40 (UV–vis) spectrophotometer with a 1 cm quartz cuvette in the range 200–800 nm. Electrochemical measurements were performed on a VersaStat-PotentioStat II cyclic voltammeter using HPLC grade acetonitrile as solvent where tetrabutylammonium perchlorate was used as supporting electrolyte at a scan rate 50 mV/s. Platinum and saturated calomel electrode (SCE) were the working and the reference electrodes in the process respectively. C, H, N microanalyses were carried out with a Perkin–Elmer 2400 II elemental analyzer. Fluorescence spectroscopic measurements were performed on a JOBIN YVON Fluoro Max 3 fluoremeter using a 10 × 10 mm^2 cuvette. Viscosity measurements were conducted on an Ubbelodhe viscometer, immersed in a thermostated water bath maintained at 298 K. The relative viscosities of the samples were determined using the

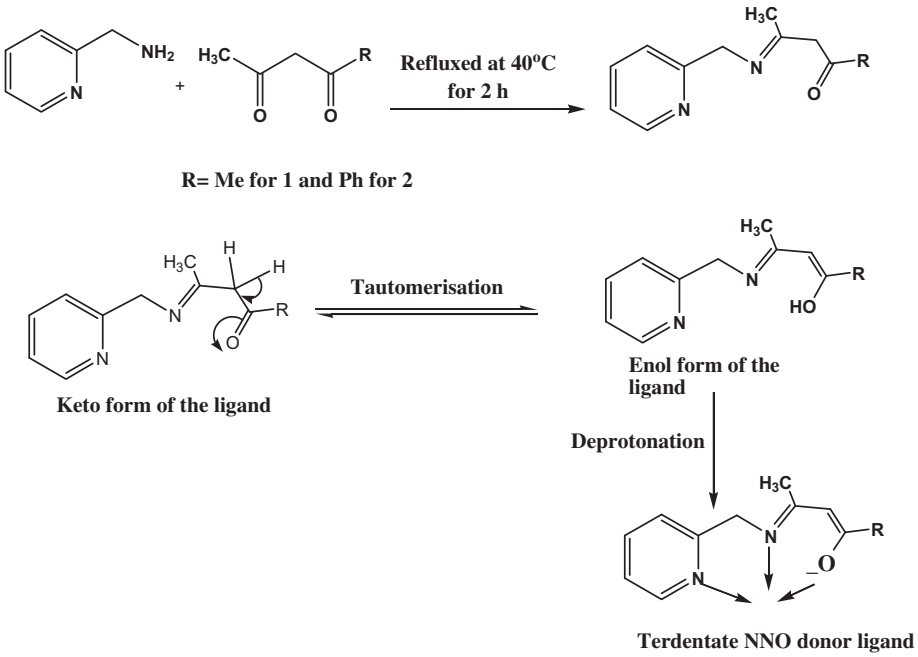

Scheme 1. Synthesis of the Schiff base ligand and its keto-enol tautomerism.

equation $\eta = (t - t_0)/t_0$, where t_0 is the flow time for buffer alone and t is the flow time of either only DNA solution or DNA solution + different concentrations of **1** and **2**.

2.4. X-ray crystallography

The X-ray diffraction experiment of **1** was carried out at 295(2) K on a brown plate shaped single crystal (0.28 mm × 0.22 mm × 0.08 mm). The intensity data of **1** were collected with a Bruker APEX-II CCD diffractometer using ω scan technique with Mo-Kα radiation (λ = 0.71073 Å). Data reduction was performed with SAINT program [29]. Empirical absorption corrections were carried out using the SADABS program [30]. The structures were solved by direct methods by using the SIR97 program [31]. All non hydrogen atoms were refined anisotropically by full-matrix least-squares based on F^2. The H atoms were generated geometrically and were included in the refinement in the riding model approximation. The lattice constants were refined by least-square refinement using 8528 total reflections ($1.9° < \theta < 25.2°$), 2757 unique reflection (R_{int} = 0.021). Structure solution and refinement based on 2451 observed reflections with $I > 2\sigma(I)$ and 258 parameters gave final R = 0.0275, wR = 0.0789 and S = 1.02. The fluorine atoms of the trifluoromethyl group are disordered over three orientations rotated about the C12–C13 bond, with occupancy factors of 0.53(3), 0.34(3) and 0.13(2), respectively. During the refinement the C–F and F···F distances were restrained to be equal and the U_{ij} components of the disordered F atoms were restrained to approximate isotropic behavior. The X-ray diffraction experiment of **2** was carried out at 100(2) K on a green needle shaped single crystal (0.08 mm × 0.18 mm × 0.62 mm). The selected crystal was mounted on a Bruker CCD area diffractometer with Mo-Kα radiation (λ = 0.71073Å). The lattice constants were refined by least-square refinement using 17,576 total reflections ($2.79° < \theta < 27.47°$), 3687 unique reflection (R_{int} = 0.0402). Structure solution and refinement based on 3039 observed reflections with $I > 2\sigma(I)$ and 245 parameters gave final R = 0.0462, wR = 0.1320 and S = 1.03. Data collection and data reduction were done with the APEX 2 suite programs [32]. All non hydrogen atoms were refined anisotropically by full-matrix least-squares based on F^2. The H atoms were generated geometrically and were included in the refinement in the riding model approximation. Selected crystallographic data, experimental conditions and relevant features of the structural refinements for both the complexes are summarized in Table 1.

2.5. Procedure of DNA binding

Binding of the complexes, **1** and **2** with calf thymus DNA (CT-DNA) was monitored by UV–vis spectroscopy and fluorescence spectroscopy in 50 mM tris–HCl/NaCl buffer (pH ~ 7.4). The concentration of the complexes in solution was 10 μM. Purity of CT-DNA was verified by the ratio of absorbance at 260 nm and 280 nm. The A_{260}/A_{280} value was between 1.8 and 1.9 indicating no further deproteinization of the DNA was required. Concentration of the DNA solution was obtained by dividing absorbance at 260 nm by the molar extinction coefficient ε_{260} = 6600 M^{-1} cm^{-1} per base for CT-DNA [33]. Therefore, in all experiments the DNA concentration has been expressed in terms of base.

For DNA binding studies the following compound-DNA equilibrium was considered

$$L + D \rightleftharpoons LD \tag{1}$$

$$K_d = [L][D]/[LD] \tag{2}$$

L represents the complexes used in the experiments while D represents CT-DNA. The apparent dissociation constant ($K_d = 1/K_{app}$ where K_{app} is the apparent binding constant) was determined using non-linear curve fit analysis [Eqs. (3) and (4)]. All experimental points for binding isotherms were fitted by least-square analysis;

$$K_d = \frac{\left[C_0 - \left(\frac{\Delta A}{\Delta A_{max}}\right)C_0\right]\left[C_D - \left(\frac{\Delta A}{\Delta A_{max}}\right)C_0\right]}{\left(\frac{\Delta A}{\Delta A_{max}}\right)C_0} \tag{3}$$

$$C_0\left(\frac{\Delta A}{\Delta A_{max}}\right)^2 - (C_0 + C_D + K_d)\left(\frac{\Delta A}{\Delta A_{max}}\right) + C_D = 0 \tag{4}$$

ΔA is the change in absorbance at 313 nm for **1** and 325 nm for **2** while ΔA_{max} is the same parameter when the respective complexes are totally bound to CT-DNA. C_D is the concentration of CT-DNA and C_0 is the initial concentration of each complex. A double reciprocal plot was used for the determination of ΔA_{max} and K_d using Eq. (5) [34]:

$$\frac{1}{\Delta A} = \frac{1}{\Delta A_{max}} + \frac{K_d}{\Delta A_{max}(C_D - C_0)} \tag{5}$$

This approach is based on the assumption that absorbance is linearly proportional to the concentration of the complexes. The concentration of the complexes was 10 μM and CT-DNA concentration was kept around 12–15-fold greater than that of the complex.

Table 1
Crystal structure parameters of **1** and **2**.

Parameters	**1**	**2**
Empirical formula	C_{13} H_{13} Cu F_3 N_2 O_3	C_{18} H_{15} Cu F_3 N_2 O_3
Formula weight	365.79	427.86
Crystal system	Triclinic	Triclinic
Space group	P-1	P-1
a (Å)	7.6843(4)	7.8075(18)
b (Å)	9.2951(5)	10.732(3)
c (Å)	11.1932(6)	10.785(3)
α (°)	93.1770(8)	97.227(9)
β (°)	104.7480(9)	108.391(7)
γ (°)	98.9368(8)	96.360(6)
V (Å^3)	759.98(7)	839.8(3)
Z	2	2
Temperature (K)	295	100(2)
$\lambda_{Mo-K\alpha}$ (Å)	0.71073	0.71073
D_c (Mg m^{-3})	1.599	1.692
μ (mm^{-1})	1.481	1.355
F (0 0 0)	370	434
θ range for data collection (°)	1.9–25.2	2.79–27.47°
Total data	8528	17,576
Unique data	2757	3687
Observed data [$I > 2\sigma(I)$]	2451	3039
R^a	0.0275	0.0462
R_w^b	0.0789	0.1320
s	1.02	1.03
R_{int}	0.021	0.0402
$\Delta\rho_{max}$ (e^-. Å^{-3})	0.30	1.33
$\Delta\rho_{min}$ (e^-. Å^{-3})	−0.13	−1.03

3. Results and discussion

3.1. Fourier transform IR spectroscopy

The IR spectra of **1** and **2** were analyzed in comparison with their free ligand **HL^1** and **HL^2** in the region 4000–400 cm^{-1}. A strong sharp absorption band around 1607 cm^{-1} in the spectrum of **HL^1** and around 1654 cm^{-1} in the spectrum of **HL^2** can be assigned to the C=N group which initially confirms the formation

of the Schiff bases. In the complexes, **1** and **2** those bands are shifted to 1574 and 1593 cm^{-1} respectively upon complexation with the metal, which can be attributed to the coordination of the nitrogen atom of the imino group to the metal ion [35]. The ligands $\mathbf{HL^1}$ and $\mathbf{HL^2}$ show well defined bands at 3410 and 3404 cm^{-1} respectively due to O—H stretching which disappear in the complexes and a C—O absorption band at 1057 cm^{-1} in both the spectra of **1** and **2** appears indicating that the ligands have undergone deprotonation on complexation. The low energy pyridine ring in plane and out of plane vibrations observed in the spectrum of $\mathbf{HL^1}$ at 604 and 628 cm^{-1} and of $\mathbf{HL^2}$ at 610 and 620 cm^{-1} respectively whereas the corresponding bands for **1** and **2** are shifted to higher frequencies which is a good indication of the coordination of the heterocyclic nitrogen [36]. The typical trifluoroacetate vibrations $\nu_{asym}(COO)$ at 1615 cm^{-1} for **1** and 1612 cm^{-1} for **2** as well as the $\nu_{sym}(COO)$ at 1356 cm^{-1} for both **1** and **2** are observed in the spectra of the complexes. The differences between $\nu_{asym}(COO)$ and $\nu_{sym}(COO)$, $\Delta\nu$ (259 and 256 cm^{-1} in **1** and **2** respectively) are much greater than 164 cm^{-1} observed in free trifluoroacetate ion indicating the presence of a deprotonated carboxylate group coordinated to the metal centers in monodentate terminal fashion [36, 37]. Sharp bands appearing at 458 and 412 cm^{-1} in the spectra of **1** and **2** respectively correspond to ν_{Cu-N} indicating the metal-nitrogen coordination.

3.2. UV–vis spectroscopy

UV–vis spectra of the free ligands and the complexes were recorded at 300 K in HPLC grade acetonitrile solution. The electronic spectral data for **1** and **2** in acetonitrile solvent are in good agreement with their geometry. The UV–vis spectra of the free ligands exhibit two charge transfer (CT) bands at 312, 270 nm in $\mathbf{HL^1}$ and at 331, 248 nm in $\mathbf{HL^2}$ which can be attributed to $n \rightarrow \pi^*$ and $\pi \rightarrow \pi^*$ transitions within the Schiff base ligands. Three distinct CT bands appeared in the spectra of the complexes at 325, 282, 234 nm in **1** and 361, 305, 244 nm in **2** which indicate that the ligand centered CT bands may have undergone large bathochromic shifts in the spectra of the complexes appearing at 325, 282 nm in **1** and 361, 305 nm in **2**. The band at 234 nm in **1** and 244 nm in **2** can be considered as $L \rightarrow M$ charge transfer transitions as those were absent in the spectra of the respective free ligands. In the spectra of the complexes, much weaker, less well defined broad bands are found at the lower energy regions associated with *d–d* transitions. **1** and **2** are assumed to have a square-planar geometry with a *d–d* transition at 595 and 600 nm respectively, similar to those observed for structurally well characterized square-planar copper(II) complexes [38].

3.3. Cyclic voltammetry

The electrochemical behavior of **1** and **2** were studied in HPLC grade acetonitrile medium with tetrabutylammonium perchlorate as supporting electrolyte at a scan rate of 50 mV sec^{-1}. **1** showed a reductive response at 0.452 V vs SCE, which is assigned to $Cu^{II} \rightarrow Cu^{I}$ reduction with no oxidative response for $Cu^{I} \rightarrow Cu^{II}$ oxidation during anodic scan suggesting that the Cu^{I} species formed during reduction is too unstable to get oxidized and may have undergone decomposition [39]. Unlike **1**, **2** showed a reductive response at +0.389 V and an oxidative response at +0.555 V for $Cu^{II} \rightarrow Cu^{I} \rightarrow Cu^{II}$ cycle. This reduction and oxidation are quasi reversible, characterized by a peak to peak separation (ΔE_p) 166 mV which remain unchanged upon changing the scan rate suggesting quasi reversible redox behavior of **2**. A distinct ligand oxidation peak appeared at +1.275 V and +1.248 V respectively for $\mathbf{HL^1}$ and $\mathbf{HL^2}$.

3.4. X-ray crystal structures of *1* and *2*

The structures of **1** and **2** have been confirmed by single crystal X-ray diffraction study. The ORTEP diagrams of the complexes are shown in Figs. 1 and 2 and selected bond distances and angles are given in Table 2. The structures of both **1** and **2** consist of mononuclear units of $[Cu\mathbf{L^1}(CF_3COO)]$ and $[Cu\mathbf{L^2}(CF_3COO)]$ where $\mathbf{HL^1}$=$CH_3C(OH)$=$CHC(CH_3)$=$NCH_2C_5H_4N$ and $\mathbf{HL^2}$=$C_6H_5C(OH)$=$CHC(CH_3)$=$NCH_2C_5H_4N$. In both complexes the copper ions have distorted square-planar geometry and are bound to the donor atoms N1, N2, O1 and O2. Out of the four coordination sites three positions are occupied by two nitrogen (pyridyl and imino) atoms and a deprotonated enolato oxygen atom of the corresponding tridentate NNO donor Schiff base $(\mathbf{L^1})^-$ and $(\mathbf{L^2})^-$. The fourth position of the square plane is occupied by one of the oxygen atoms (O2) of a trifluoroacetate ion coordinated to the central copper atom in terminal fashion. The Cu1—O2 distance is 1.9653(15) Å in **1** and 1.961(2) Å in **2** and matches well with the reported data of other copper(II)-monodentate trifluoroacetato complexes [40, 41]. The geometry around the Cu1 square plane suffers distortion which is evident from the chelate bite angles made by the NNO donor set of the respective ligands in both the complexes. The N1—Cu1—N2 angles [83.52(7)° in **1** and 84.17(10)° in **2**] undergo compression whereas the O1—Cu1—N2 angles [94.80(7)° in **1** and 94.44(10)° in **2**] undergo expansion from their ideal 90° value

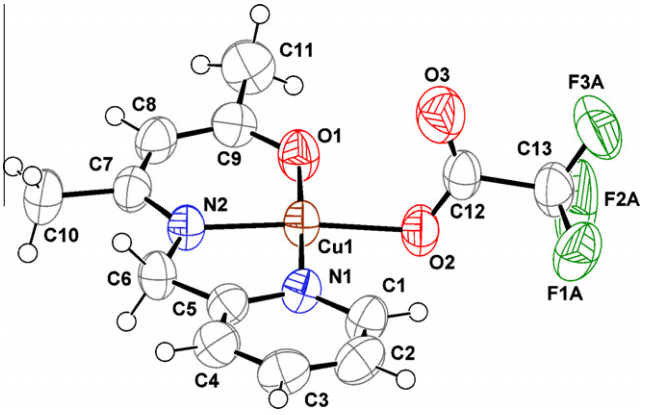

Fig. 1. An ORTEP drawing of **1** with displacement ellipsoids drawn at the 50% probability level. Only the major component of disorder affecting the triflurometyl group is shown.

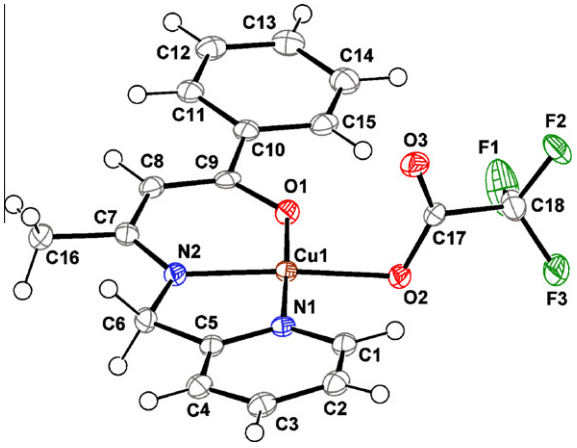

Fig. 2. An ORTEP drawing of **2** with displacement ellipsoids drawn at the 50% probability level.

Table 2
Selected bond lengths (Å) and bond angles (°) for **1** and **2**.

Bond lengths (Å)	1	2
Cu1—O1	1.8905(15)	1.879(2)
Cu1—O2	1.9653(15)	1.961(2)
Cu1—N1	1.9912(17)	1.963(3)
Cu1—N2	1.9141(17)	1.919(2)
Bond angles (°)		
O1—Cu1—O2	88.91(7)	86.29(9)
O1—Cu1—N1	176.85(7)	176.39(8)
O1—Cu1—N2	94.80(7)	94.44(10)
O2—Cu1—N1	92.96(7)	95.37(9)
O2—Cu1—N2	174.66(7)	175.31(8)
N1—Cu1—N2	83.52(7)	84.17(10)

[11] and this behavior is expected because the compressed and expanded bite angles are enclosed by a five membered and a six membered chelate rings respectively. The transoid angles [ranging from 174.66(7)° to 176.85(7)° in **1** and from 175.31(8)° to 176.39(8)° in **2**] also deviate from the ideal value for a square planar system. The Cu1—N1 bond length of **1** [1.9912(7) Å] is slightly longer than that of **2** [1.963(3) Å]. This behavior can be explained by the fact that in **2** the N1—Cu1—N2 bond angle [84.17(10)°] is closer to the ideal value (90°) than the angle in **1** [83.52(7)°] which is responsible for better overlap of the Cu-d and N-p orbitals in **2** resulting in shorter Cu1—N1 bond distance. The N2—Cu1—O1 bond angles in both **1** and **2** have quite similar values, the Cu1—N2 bond lengths [1.9141(17) Å in **1** and 1.919(2) Å in **2**] are comparable indicating same extent of $d\pi$–$p\pi$ orbital overlap of the Cu1—N2 bonds.

Earlier Mitra and his group have synthesized a few mononuclear copper(II) complexes with the same Schiff base ligand system of **1** [11] and **2** [12] with similar structural features but different coordinating non chelating anions. Both complexes **1** and **2** are almost planar. The deviation of the Cu1 atom above the mean square plane [0.0108(2) Å in **1** and 0.0120(4) Å in **2**] is much smaller than those observed in the copper(II) complexes reported earlier [11–12]. Moreover the angles between the planes defined by Cu1, N1, N2 and Cu1, N2, O1 are 2.68(6)° and 3.34(8)° respectively, in **1** and **2**, much smaller than that in similar copper(II) complexes [11] indicating much less tetrahedral distortion for **1** and **2** from perfect square-planar geometry.

Centrosymmetrically-related mononuclear units of **1** and **2** are interconnected by H-bonding interactions to form dimers. The H-bonding data are presented in Table 3. The H-bonded dimeric structures of **1** and **2** are shown in Figs. 3 and 4 respectively. Crystal packing diagrams for the two complexes are depicted in Figs. 5 and 6 respectively. Though the intermolecular H-bond acceptors in both the complexes are provided by the same oxygen atom (O3) of the trifluoroacetate anion, the donor hydrogens are different due to the difference in spatial orientation of the mononuclear units resulting in bifurcated H-bonding in **1**. In **2** the methylene proton (H8) belonging to the benzoyl acetone part of $(\mathbf{L^2})^-$ is the sole H-bond donor whereas in **1** the methylene proton (H6B) belonging

Table 3
H-bond parameters of **1** and **2**.

	D—H···A	d(D—H) Å	d(H···A) Å	d(D···A) Å	<(DHA)°
1	C1—H1···O2	0.93	2.55	3.051(3)	114
	C4—H4···O3	0.93	2.59	3.312(3)	134
	C6—H6B···O3	0.97	2.54	3.316(3)	137
2	C1—H1···O2	0.95	2.58	3.087(4)	114
	C8—H8···O3	0.95	2.43	3.302(4)	152

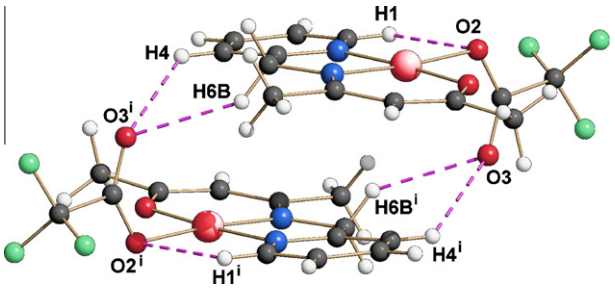

Fig. 3. The dimeric unit of **1** formed by intermolecular C—H···O hydrogen bonds (dashed lines). Intramolecular H bonds are also shown. Only the major component of disorder is shown. Symmetry code: (i) 2−x, −y, 2−z.

to the 2-picolyl amine part of $(\mathbf{L^1})^-$ along with one aromatic proton (H4) of the pyridyl moiety are close enough to O3 to act as H-bond donor. In both complexes a similar intramolecular C—H···O H-bond involving the O2 oxygen atom and the aromatic H1 hydrogen atom is observed.

3.5. Results of DNA binding

3.5.1. Absorbance spectroscopic study to determine the binding constants of *1* and *2*

The ability of the complexes (**1** and **2**) to bind with calf thymus DNA (CT-DNA) was investigated by UV–vis absorption spectroscopy at physiological pH (7.4). Prior to titration of the complexes with CT-DNA their stability was checked in 50 mM tris–HCl/NaCl buffer (pH 7.4) at room temperature for 24 h which was then monitored by UV–vis spectroscopy. No liberation of ligands was observed under the above-mentioned conditions indicating that the complexes are very stable in the said medium. In tris-buffer **1** and **2** showed charge transfer bands at 313 and 325 nm respectively.

In order to measure the strength of binding of the complexes to CT-DNA 10 μM solutions of **1** and **2** in tris-buffer were titrated with increasing concentration of CT-DNA (0–140 μM) and the change in absorbance intensities at 313 nm for **1** and 325 nm for **2** were observed. In both cases the bands showed appreciable degree of hypochromism (Figs. 7 and 8) but in case of **1** saturation was reached much earlier than **2**. From the spectral changes the apparent binding constants (K_{app}) were calculated by regression analyses using Eqs. (4) and (5) (under Section 2.5.) for both complexes **1** and **2** as shown in Figs. 9 and 10 respectively. The K_{app} values obtained from UV–vis and fluorescence studies by applying different methods of analysis are summarized in Table 4. It is therefore clear from the DNA binding constants of the complexes that **1** ($K_{app} = 2.61 \times 10^4\ M^{-1}$) has a greater affinity for binding to calf thymus DNA in comparison to **2** ($K_{app} = 1.54 \times 10^4\ M^{-1}$).

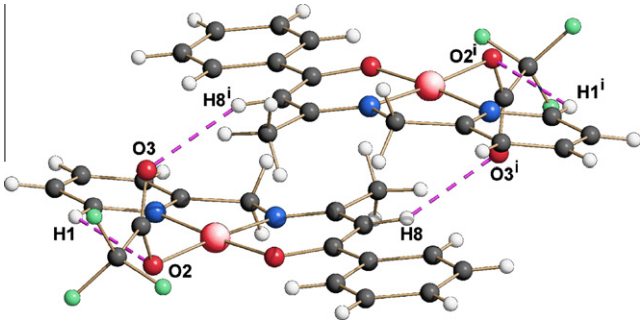

Fig. 4. The dimeric unit of **2** formed by intermolecular C—H···O hydrogen bonds (dashed lines). Intramolecular H bonds are also shown. Symmetry code: (i) 1−*x*, 2−*y*, −*z*.

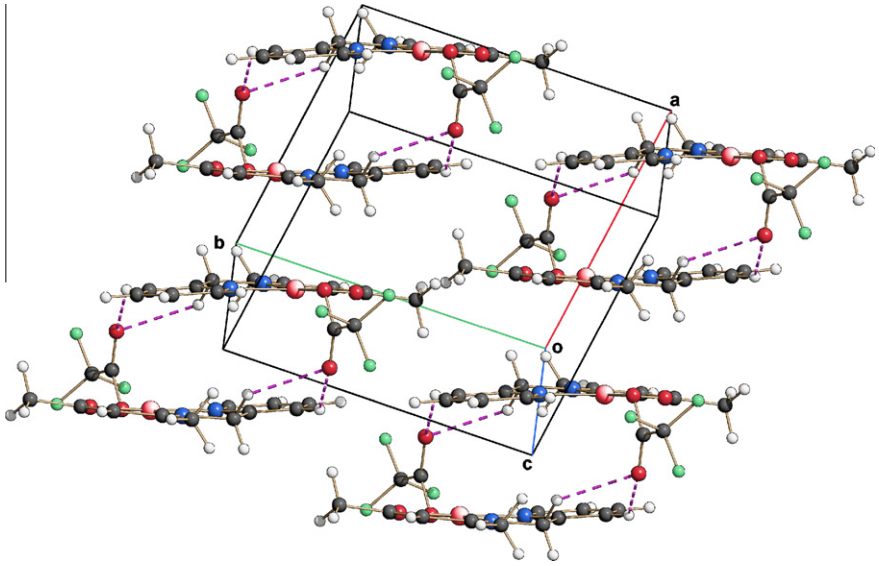

Fig. 5. The crystal packing of **1** showing intermolecular hydrogen-bonding interactions as dashed lines. Only the major component of disorder is shown.

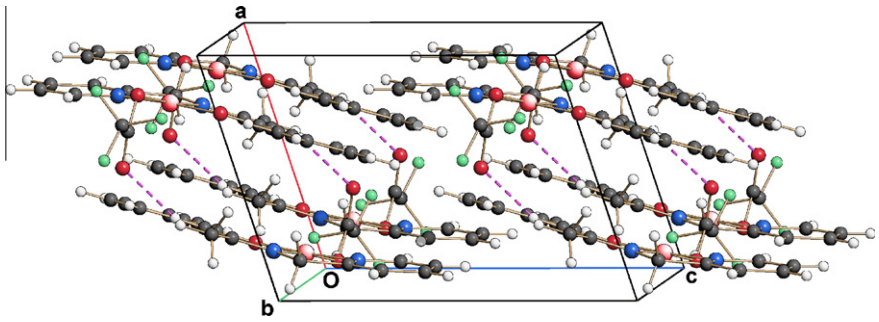

Fig. 6. The crystal packing of **2** showing intermolecular hydrogen-bonding interactions as dashed lines.

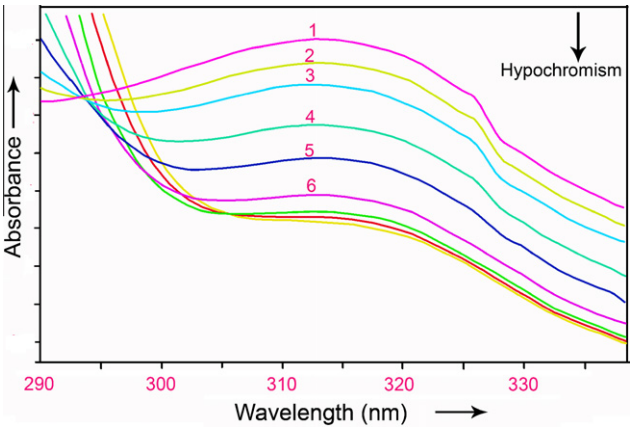

Fig. 7. Change in absorption spectra of **1** on titration with increasing CT-DNA concentration.

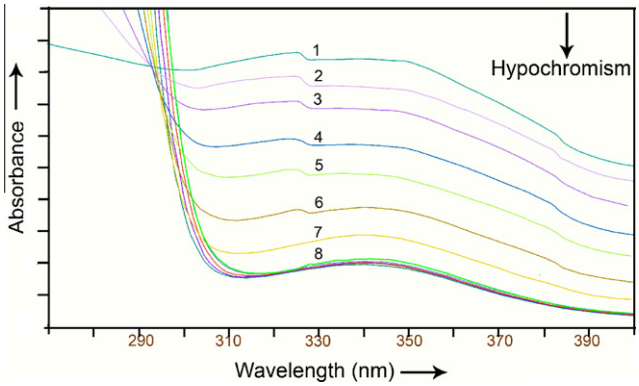

Fig. 8. Change in absorption spectra of **2** on titration with increasing CT-DNA concentration.

3.5.2. Fluorescence spectroscopic study

In order to see whether **1** and **2** interact with calf thymus DNA, solution of the complexes at physiological pH (7.4) was titrated with increasing amount of CT-DNA keeping concentration of **1** and **2** unchanged during such titration. For this purpose separate solutions were made containing constant concentration of complexes and different concentrations of CT-DNA. The fluorescence spectra of **1** in presence of different amount of calf thymus DNA was recorded following an excitation at 220 nm. The emission spectrum exhibits a maximum at 405 nm. From Fig. S1 (provided as a supplementary data), it is clear that fluorescence emission intensity decreased gradually with increasing amount of calf thymus DNA showing that fluorescence of **1** got sufficiently quenched upon binding to DNA.

The binding isotherms were analyzed using non-linear curve fitting following equilibrium (1) [42]. Apparent dissociation

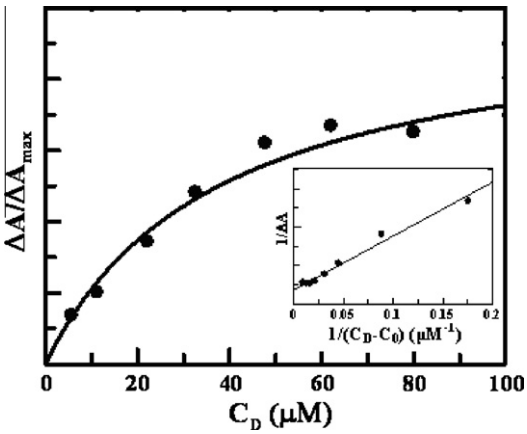

Fig. 9. Plot of non-linear variation of $\Delta A/\Delta A_{max}$ with increasing concentration of DNA using UV–vis titration method for **1**. The inset shows the double reciprocal plot of interaction of **1** with CT-DNA.

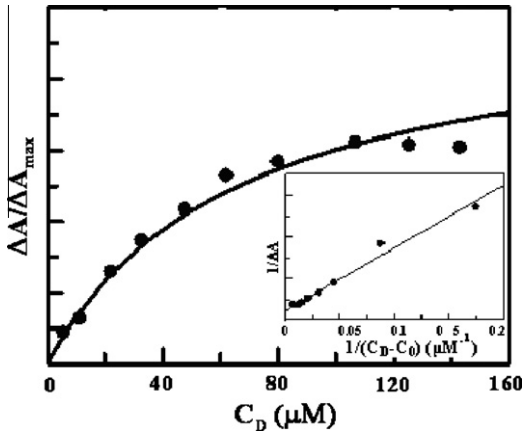

Fig. 10. Plot of non-linear variation of $\Delta A/\Delta A_{max}$ with increasing concentration of DNA using UV–vis titration method for **2**. The inset shows the double reciprocal plot of interaction of **2** with CT-DNA.

constant ($K_d = 1/K_{app}$, where K_{app} is the apparent binding constant) was determined using non-linear curve fit analysis [Eqs. (6) and (7)] based on such equilibrium. All experimental points for binding isotherms were fitted according to least-square analysis;

$$K_d = \frac{\left[C_0 - \left(\frac{\Delta F}{\Delta F_{max}}\right)C_0\right]\left[C_D - \left(\frac{\Delta F}{\Delta F_{max}}\right)C_0\right]}{\left(\frac{\Delta F}{\Delta F_{max}}\right)C_0} \quad (6)$$

$$C_0\left(\frac{\Delta F}{\Delta F_{max}}\right)^2 - (C_0 + C_D + K_d)\left(\frac{\Delta F}{\Delta F_{max}}\right) + C_D = 0 \quad (7)$$

where ΔF is the change in fluorescence emission intensity of **1** at 405 nm (λ_{ex} = 220 nm) for each point of the titration curve, ΔF_{max} is the same parameter when **1** is totally bound to CT-DNA, C_D is the concentration of CT-DNA and C_0 is the initial concentration of

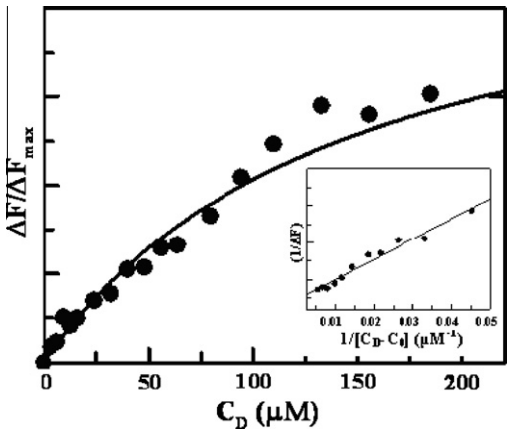

Fig. 11. Plot of non-linear variation of $\Delta F/\Delta F_{max}$ with increasing concentration of DNA using fluorescence titration method for **1**. The inset shows the double reciprocal plot of interaction of **1** with CT-DNA.

1. Double reciprocal plot (Fig. 11 inset) was used for the determination of ΔF_{max} and K_d using the following equation:

$$\frac{1}{\Delta F} = \frac{1}{\Delta F_{max}} + \frac{K_d}{\Delta F_{max}(C_D - C_0)} \quad (8)$$

This approach is based on the assumption that fluorescence is linearly proportional to the concentration of **1**, the concentration of which was 10 μM while CT-DNA concentration toward the end of the titration was around 20-fold greater than that of the complex in solution.

Fig. 11, which shows the binding isotherms of **1** with CT-DNA was used to calculate the binding constant [Eqs. (6) and (7)] as described above. The apparent binding constant obtained was $0.74 \times 10^4\ M^{-1}$. The apparent binding constant obtained from double reciprocal plot following Eq. (8) [Fig. 11 inset] was $0.80 \times 10^4\ M^{-1}$. The values indicate that the apparent binding constants obtained from two different methods of analysis are similar.

2, which has a λ_{max} at 325 nm was excited at 340 nm using a fluorescence spectrophotometer. The emission spectra which were recorded from 500 nm to 700 nm did not show any characteristic peak that could be used to monitor any possible interaction with CT-DNA, for which reason interaction of **2** could not be followed by fluorescence spectroscopy.

3.5.3. Viscosity measurement

Optical or photophysical investigations are necessary but not sufficient to establish the mode of binding between metal complexes and DNA. In absence of crystallographic information, hydrodynamic methods are proved to be least ambiguous to support a complex-DNA binding model [43] as these measurements are very much sensitive to length change (i.e. viscosity and sedimentation). When a substance intercalates between DNA base pairs it unwinds the DNA helix and hence increases the overall DNA contour length resulting in significant increase in the viscosity of DNA solution. In contrast, non classical interaction that bend (or kink) the DNA helix reduce its effective length and concomitantly its viscosity.

Table 4
The K_{app} values obtained from UV–vis and fluorescence studies by applying different methods of analysis.

Methods of analysis	UV–vis		Fluorescence	
	Double reciprocal fit	Non-linear fit	Double reciprocal fit	Non-linear fit
1	$2.61 \times 10^4\ M^{-1}$	$2.65 \times 10^4\ M^{-1}$	$0.80 \times 10^4\ M^{-1}$	$0.74 \times 10^4\ M^{-1}$
2	$1.54 \times 10^4\ M^{-1}$	$1.51 \times 10^4\ M^{-1}$	–	–

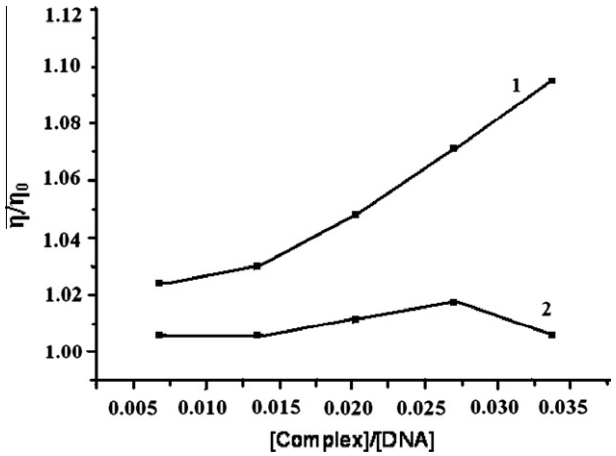

Fig. 12. The plot showing the effect of increasing concentrations of **1** and **2** on the viscosity of DNA.

Moreover binding of a molecule to the surface or groove of the DNA helix produces no significant change in DNA solution-viscosity [13]. The effects of **1** and **2** on the viscosity of CT-DNA are shown in Fig. 12. The relative viscosity of the DNA solution has increased gradually on addition of increasing concentration of **1** but with the increasing concentration of **2** it has not shown any significant change. Thus **1** is found to show intercalative mode of binding like that of the proven intercalator ethidium bromide. In contrast, **2** being bulkier than **1** is a less effective intercalator and may have bound exclusively to the DNA grooves like that of netropsin, distamycin etc. or to the surface of the DNA helix causing less pronounced change in DNA solution-viscosity.

3.5.4. Discussions

From the DNA binding studies it is evident that **1** binds with DNA more strongly compared to **2**. Moreover **1** is a good intercalator whereas **2** shows groove binding characteristics. Such behavior of the complexes can be interpreted highlighting the difference in substituents on the ligands used in the two complexes. The presence of a methyl group at the C9 position in **1** which in **2** is phenyl (Figs. 1 and 2) may be thought to be a source of difference in reactivity. The presence of a phenyl ring should promote the possibility of intercalation [44] but here the situation is reverse. The methyl group at the C9 position in **1** has induced more planarity within the complex compared to the phenyl group attached to the same position in **2** which is evident from the X-ray crystallography data. The relative displacement of the C9 atom holding the methyl and the phenyl groups in **1** and **2** respectively from the mean plane passing through N1, N2, O1 and O2 is 0.093 Å in **1** whereas 0.225 Å in **2**. Thus comparatively smaller deviation of **1** from planarity compared to **2** makes it a good DNA intercalator.

4. Conclusion

Though the complexes, **1** and **2** are isostructural their H-bonding patterns are quite different due to the difference in spatial orientation of two centrosymmetrically-related mononuclear units. From the spectroscopic titration results it is evident that **1** has greater DNA binding ability than **2**, probably due to the presence of the methyl substituent attached to C9 of $\mathbf{HL^1}$ which is less bulkier, less electron rich and more planar than the phenyl substituent attached to C9 of $\mathbf{HL^2}$. The phenyl group reduces the ability of **2** to bind with DNA bases though the reverse should be expected. From the viscosity measurement it is clear that **1** binds with DNA by intercalative method whereas **2** shows surface/groove binding. Thus the complexes obtained by varying only an alkyl substituent in the ligand fragment have shown much difference in their H-bonding features as well as in their biochemical activities.

Acknowledgements

D. Sadhukhan is thankful to University Grants Commission, New Delhi, Government of India and A. Ray acknowledges Council of Scientific and Industrial Research, New Delhi, Govt. of India for providing them financial support to carry out the work. The authors are also thankful to Mr. Partha Sarathi Guin of Saha Institute of Nuclear Physics, Kolkata, India for helping in the fluorescence study.

Appendix A. Supplementary material

Supplementary data associated with this article can be found, in the online version, at doi:10.1016/j.molstruc.2010.04.034.

CCDC numbers for **1** and **2** are 754,875 and 664,113. These data can be obtained free of charge at www.ccdc.cam.ac.uk (or from Cambridge Crystallographic Data Centre, 12, Union Road, Cambridge CB2 1EZ, UK; email: deposit@ccdc.cam.ac.uk). The supplementary data also contains Fig. S1 (plot of fluorescence intensity vs wave length for **1**).

References

[1] C.O. Rodriguez de Barbarin, N.A. Bailey, D.E. Fenton, Q.-Y. He, J. Chem. Soc., Dalton Trans. (1997) 161.
[2] Y.Y. Chen, D.E. Chu, B.D. McKinney, L.J. Willis, S.E. Cummings, Inorg. Chem. 20 (1981) 1885.
[3] J. Ribas, M. Monfort, I. Resino, X. Solans, P. Rabu, F. Maingot, M. Drillan, Angew. Chem., Int. Ed. Engl. 35 (1996) 2520.
[4] R. Vicente, A. Escuer, E. Penalba, X. Solans, M. Font-Badia, J. Chem. Soc., Dalton Trans. (1994) 3005.
[5] R. Vicente, A. Escuer, J. Ribas, X. Solans, J. Chem. Soc., Dalton Trans. (1994) 259.
[6] J. Ribas, C. Diaz, X. Solans, M. Font-Bardia, J. Chem. Soc., Dalton Trans. (1997) 35.
[7] R.J. Doedens, Prog. Inorg. Chem. 21 (1976) 209.
[8] S.J. Rettig, R.C. Thompson, J. Trotter, S. Xia, Inorg. Chem. 38 (1999) 360 (and references therein).
[9] H.V. Huynh, D.L. Van, F.E. Hahn, T.S.A. Hor, J. Organomet. Chem. 689 (2004) 1766.
[10] Y.-Y. Wang, Q. Shi, Q.-Z. Shi, Y.-C. Gao, Z.-Y. Zhou, Polyhedron 18 (1999) 2009.
[11] R. Karmakar, C. Roy Choudhury, A.S. Batsanov, S.R. Batten, S. Mitra, Struct. Chem. 16 (2005) 535.
[12] A. Ray, G. Pilet, C.J. Gomez-Garcia, S. Mitra, Polyhedron 28 (2009) 511.
[13] S. Banerjee, S. Mondal, W. Chakraborty, S. Sen, R. Gachhui, R.J. Butcher, A.M.Z. Slawin, C. Mandal, S. Mitra, Polyhedron 28 (2009) 2785.
[14] L. Li, K.D. Karlin, S.E. Rokita, J. Am. Chem. Soc. 127 (2005) 520.
[15] J.-H. Li, J.-T. Wang, P. Hu, L.-Y. Zhang, Z.-N. Chen, Z.-W. Mao, L.-N. Ji, Polyhedron 27 (2008) 1898.
[16] D. Kong, J. Reibenspies, J. Mao, A. Clearfield, A.E. Martell, Inorg. Chim. Acta 342 (2003) 1568.
[17] L.M. Rossi, A. Neves, R. Hörner, H. Terenzi, B. Szpoganicz, J. Sugai, Inorg. Chim. Acta 337 (2002) 366.
[18] K.J. Humphreys, K.D. Karlin, S.E. Rokita, J. Am. Chem. Soc. 124 (2002) 6009.
[19] G.N. De Iuliis, G.A. Lawrance, S. Fieuw-Makaroff, Inorg. Chem. Commun. 3 (2000) 307.
[20] L. Zhu, O. dos Santos, C.W. Koo, M. Rybstein, L. Pape, J.W. Canary, Inorg. Chem. 42 (2003) 7912.
[21] S.-P. Tang, L. Hou, Z.-W. Mao, L.-N. Ji, Polyhedron 28 (2009) 586.
[22] M.C. Prabhakara, B. Basavaraju, H.S. Bhojya Naik, Bioinorg. Chem. Appl. 2007 (2007) 36497.
[23] Y. Wang, G. Lin, J. Hong, T. Lu, L. Li, N. Okabe, M. Odoko, Inorg. Chim. Acta 362 (2009) 377.
[24] A.M. Thomas, A.D. Naik, M. Nethaji, A.R. Chakravarty, Inorg. Chim. Acta 357 (2004) 2315.
[25] J.D. Ranford, P.J. Sadler, D.A. Tocher, J. Chem. Soc., Dalton Trans. (1993) 3393.
[26] M.J. Plater, M.R. St, J. Foreman, J.M.S. Skakle, R.A. Howie, Inorg. Chim. Acta 332 (2002) 135.
[27] C.A. Johns, G.M. Golzar Hossain, K.M. Abdul Malik, S. Zahir Haider, U.K. Rowzatur Romman, Polyhedron 20 (2001) 721.
[28] S. Banerjee, S. Mondal, S. Sen, S. Das, D.L. Hughes, C. Rizzoli, C. Desplanches, C. Mandal, S. Mitra, Dalton Trans. (2009) 6849 (and references therein).
[29] SAINT V 4.035 Software for the CCD Detector System, Siemens Analytical Instruments Division, Madison, WI, 1995.
[30] SADABS, Program for Absorption Corrections using Siemens CCD based on the Method of Bob Blessing, Acta Crystallogr. A51 (1995) 33.

[31] A. Altomare, M.C. Burla, M. Camalli, G. Gascarano, G. Giacovazzo, A.G.G. Moliterni, G. Polidori, R. Spagna, J. Appl. Crystallogr. 32 (1999) 115.
[32] Apex2 Version 2.1: Area Detector Control and Integration Software, v. 5.629 and 6.45, Bruker Analytical X-Ray Instruments, Inc., Madison, WI, USA, 2003, 2006.
[33] M.E. Reichmann, S.A. Rice, C.A. Thomas, P. Doty, J. Am. Chem. Soc. 76 (1954) 3047.
[34] S. Roy, R. Banerjee, M. Sarkar, J. Inorg. Biochem. 100 (2006) 1320.
[35] M. Dolaz, M. Tümer, M. Diğrak, Transition Met. Chem. 29 (2004) 528.
[36] K. Nakamoto, Infrared and Raman Spectra of Inorganic and Coordination Compounds, fifth ed., Theory and Applications in Inorganic Chemistry, John Wiley and Sons Inc., New York, 1997.
[37] M.T.H. Tarafder, A. Kasbollah, K.A. Crouse, A.M. Ali, B.M. Yamin, H.-K. Fun, Polyhedron 20 (2001) 236.
[38] A.B.P. Lever, Inorganic Electronic Spectroscopy, Elsevier, Amsterdam, 1984. p. 553.
[39] S. Basak, S. Sen, S. Mitra, C. Marschner, W.S. Sheldrick, Struct. Chem. 19 (2008) 115.
[40] T. Nakamura, H. Higuchi, K. Izutsu, Bull. Chem. Soc. Jpn. 62 (1989) 3089.
[41] R.L. Paul, S.M. Couchman, J.C. Jeffery, J.A. McCleverty, Z.R. Reeves, M.D. Ward, J. Chem. Soc., Dalton Trans. (2000) 845.
[42] P.S. Guin, S. Das, P.C. Mandal, J. Inorg. Biochem. 103 (2009) 1702.
[43] V.G. Vaidyanathan, B.U. Nair, J. Inorg. Biochem. 93 (2003) 271.
[44] M. Cusumano, A. Giannetto, J. Inorg. Biochem. 65 (1997) 137.